

NUMERICAL SIMULATION STUDY ON FACTORS AFFECTING THE PRE-CO₂ FRACTURING EFFECT IN SHALE OIL RESERVOIRS: A CASE STUDY ON KONG-2 MEMBER IN CANGDONG SAG, CHINA

by

Shun-Yao SONG^a, Xue-Wei **LIU^b**, Yong-Qiang **FU^b**, Yu-Xi **ZANG^c**, Hai-Zhu **WANG^{c,*}**,
Fu-Chun **TIAN^b**, Li-Fei **SHAO^b**, Yun-Peng **JIA^b**, Tao **ZHAO^b**, Qi-Wu **YIN^b**

^aNew Project Division of PetroChina Dagang Oilfield Company, Tianjin 300280, China

^bPetroleum Engineering Research Institute, PetroChina Dagang Oilfield Company, Tianjin, 300280, China

^cNational Key Laboratory of Petroleum Resources and Prospecting, China University of Petroleum (Beijing), Beijing 102249, China

A novel procedure has emerged in recent years within oilfields – namely, the utilization of a hybrid fracturing method employing pre-CO₂ injection along with sand-carry slick water. In this paper, based on the real logging data of shale oil reservoirs in the second member of Cangdong Sag, Huanghua Depression, combined with the GOHFER, a coupled three-dimensional hydraulic fracture propagation model is proposed. This research delves into an examination of how engineering factors exert their influence on the process of fracture propagation. The quantitative analysis is conducted encompassing critical fracture parameters such as half-length, height, and width, and self-defined fracture seepage area and fracture front fractal dimension. The research findings indicate that as injection displacement increases, the fracture shape undergoes a transformation from being "long, low, and wide" to becoming "short, high, and narrow".

Key words: supercritical carbon dioxide, hydraulic fracturing, shale oil reservoir, mechanical properties, simulation

Introduction

Hydraulic fracturing, a prevalent technique, is widely employed to enhance the recovery of unconventional oil and gas resources [1]. In recent times, a shift towards carbon-free strategies has accentuated the appeal of supercritical CO₂ (SC-CO₂) within the research community [2]. SC-CO₂ boasts attributes such as minimal viscosity, superior fluidity, and almost negligible surface tension. This unique trait translates to reduced rock fracture

*Corresponding author; e-mail: whz0001@126.com

pressures and the formation of intricate fracture network configurations [3, 4]. In recent years, researchers have proposed a solution in the form of blending CO₂ with water-based fracturing fluids [5]. Within this approach, CO₂ is primarily employed as a pre-fracturing fluid, with its main function being the timely replenishment of formation energy. The subsequent introduction of sand-laden water-based fracturing fluid serves to reinforce the fractures, ultimately reducing the flow resistance of reservoir fluids [6].

The exploration of hydraulic fracturing fracture propagation has predominantly involved two primary methodologies: laboratory experiments and numerical simulations. Laboratory experiments offer an intuitive approach, affording researchers the ability to directly observe and quantify the expansion of cracks under controlled conditions. Zang developed a unique triaxial fracturing visualization setup. Integrated with high-speed cameras and digital image correlation (DIC) technology, this apparatus enabled the in-depth investigation of the dynamic fracture propagation process across diverse fracturing fluid types [7]. The application of numerical simulation methods has emerged as an effective approach for conducting fracturing simulations on a field scale. There remains a significant research gap in comprehensively understanding the field-scale propagation of pre-CO₂ hybrid fracturing, considering the actual reservoir heterogeneity.

The paper commences by conducting an in-depth analysis of the geological attributes characterizing the shale oil reservoir within the Kong 2 member of the designated Cangdong sag. Subsequently, a GOHFER numerical simulation model accounting for the reservoir's inherent heterogeneity is constructed. The study then aims to an exploration of the impacts of engineering factors on the fracture propagation. Finally, a design chart of fracturing construction parameters is proposed.

Geological Setting and Construction Parameters

The Guanye 5-3-6H is situated within the Kong 2 Member of the Cangdong Sag. The predominant pore structure is attributed to matrix pores, accompanied by a minor proportion of micro-cracks. The porosity spectrum spans from 1.0% to 12.0%. The Poisson's ratio of the formation is 0.24, the Young's modulus is 28 GPa. The target zone for fracturing in this well spans 1850 m. In order to improve the degree of reservoir stimulation, the target zone for fracturing is divided into 37 sections and 222 clusters for fracturing. The section length is 50m, 6 clusters in a single section, and the spacing between clusters is 8m. Within this framework, the sections with double-numbered designations undergo a pre-CO₂ energy enhancement procedure, with each of these sections being injected with 150 m³ of CO₂. The injection is performed at a construction displacement rate of approximately 2.5 m³/min.

Mathematical Model Setup

GOHFER 3D is harnessed to forecast the fracture propagation attributes inherent to pre-CO₂ hybrid fracturing [8, 9]. Recognizing the limitations in the available drilling data for the target horizontal well Guanye 5-3-6H, the LAS logging data files from adjacent vertical wells within the same geographical region are harnessed for the purpose of geological simulation. As illustrated in Fig. 1, a 3D heterogeneous geological model measuring 1064.4 m in length, 500 m in width, and 100.8 m in height is meticulously constructed. In a bid to optimize the balance between simulation accuracy and computational efficiency, the chosen representative horizontal wells in this study adopt one single-stage 6-cluster pre-CO₂ hybrid

fracturing technique.

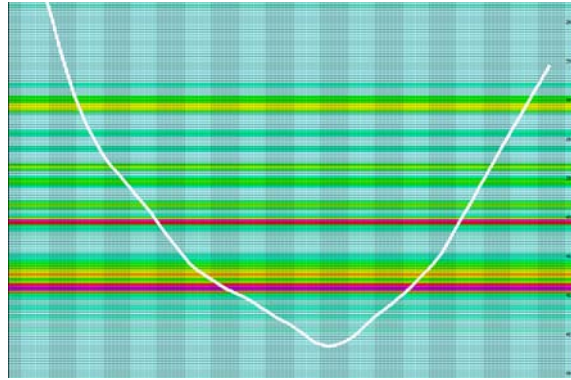


Figure 1. Numerical model geological parameters (taking permeability as an example)

Numerical Simulation Scheme

The intricate process of crack propagation induced by pre-CO₂ hybrid fracturing within shale reservoirs presents a complex phenomenon. This oilfield fracturing process is subject to the interplay of two primary influencing factors: i) Geological parameters; ii) Engineering parameters. In the context of this study, the target reservoir remains constant, thus rendering geological parameters as fixed constants. Accordingly, adaptations are implemented based on the specific operational conditions of the oilfield site, culminating in the formulation of the simulation framework outlined in Table 1.

Table 1. Simulation framework

Case	Fluid type	Injection rate (m ³ /min)	Injection volume (m ³)
1-5	CO ₂ -water	2/3/4/5/6-14	150-1700
6-9	CO ₂ -water	3-14	100/150/200/250/300-1700

Results and Discussion

Through a comprehensive comparative analysis of hydraulic fractures' half-length, width, and height under diverse operational conditions, we conduct a rigorous quantitative assessment of the impact of various engineering parameters on the fracture propagation. Furthermore, we introduce two distinct quantitative evaluation metrics: the seepage area (S) of the fracture surface, serving as an indicator of interior fracture complexity; and the fractal dimension (D), which offers a measure of the intricacy of the fracture front, as illustrated in Fig. 2.

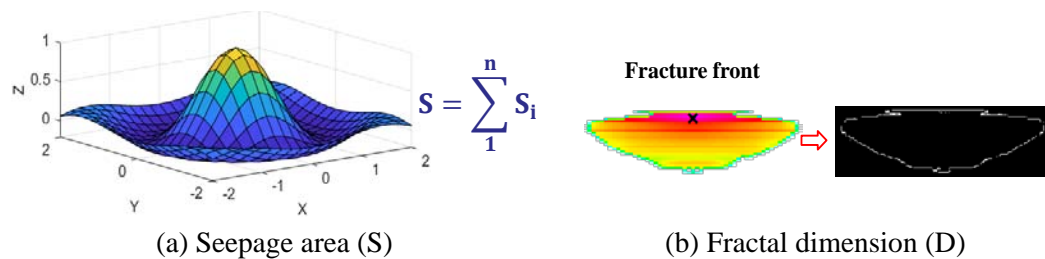


Figure2. Schematic diagram of seepage area (S) and fractal dimension (D)

Analysis of the Pre-CO₂ Injection Displacement

This study conducts numerical simulations encompassing pre-CO₂ injection displacements ranging from 2 to 6 m³/min. The initial CO₂ injection volume remained constant

at 150 m³, subsequent injection of water-based fracturing fluid occurred at a displacement of 14 m³/min, with a total volume of 1700 m³. The fracture dimensions of the six perforation clusters within the designated section are quantified and averaged to discern underlying patterns, as shown in Fig. 3. Notably, when the displacement is 3 m³/min, the maximum average half length measures 78.06 m, presenting a 2.8% increment compared to the minimum displacement value. This trend is mirrored in the crack width. The fracture height exhibits a non-linear increase trend, with its peak expansion occurring at a displacement of 3 m³/min.

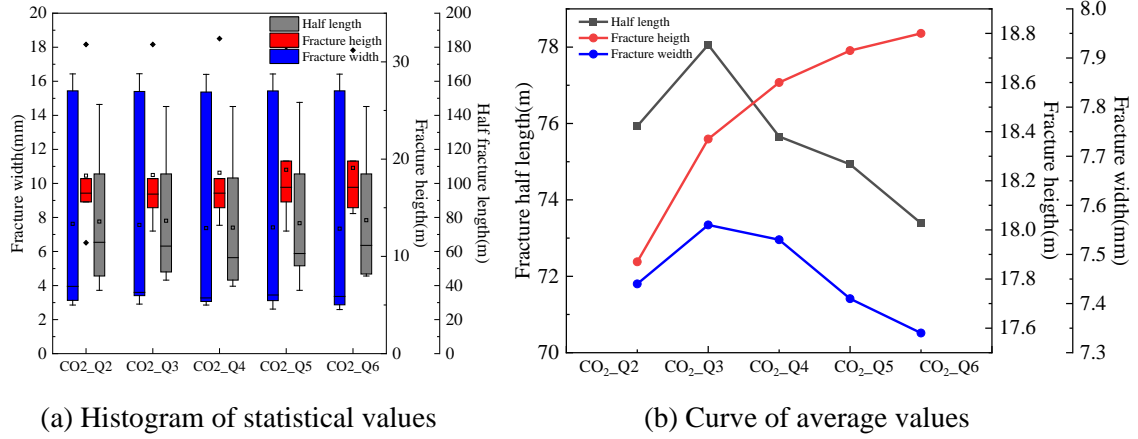


Figure3. The fracture size under different CO₂ injection displacement

As the pre-CO₂ injection displacement rises, both the *S* and the *D* exhibit an initial increase followed by a subsequent decrease. This trend is most pronounced when the displacement is 3 m³/min, at which point both parameters attain their peak values. Specifically, the *S* expands to 186432.8 m², while the *D* reaches 1.212.

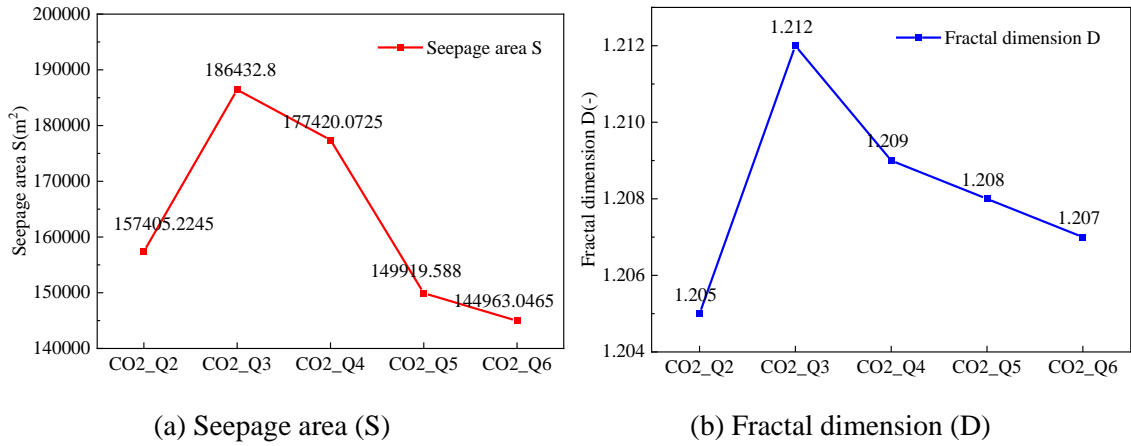


Figure4. Seepage area and fractal dimension under different CO₂ injection displacement

As the injection displacement increases, the configuration of fractures evolves from being "long, low, and wide" to "short, high, and narrow" accompanied by a diminishing trend in fracture complexity. This phenomenon arises due to the inherent attributes of CO₂, such as its low viscosity and interfacial tension. These properties facilitate the facile penetration of CO₂ into the minuscule pores of the reservoir at lower displacements, promptly rejuvenating the reservoir's energy. Nonetheless, once the CO₂ injection displacement surpasses a certain threshold, higher injection displacements expedite the formation's energy replenishment per unit time. This acceleration subsequently intensifies flow friction resistance within fractures.

Concurrently, the injected CO₂ faces limitations in infiltrating the minuscule pores of the reservoir due to the rapid displacement. Hence, it is advisable to maintain a lower pre-CO₂ injection displacement.

Analysis of the Pre-CO₂ Injection Volume

In this section, we conduct quantitative comparisons involving average fracture length, width, and height across injection volumes of 100, 150, 200, 250, and 300 m³. These comparative findings are visually depicted in Fig. 5. The discernible trend reveals that the fracture dimensions exhibit an initial increase followed by a subsequent nonlinear decline as the pre-CO₂ injection volume escalates. Notably, the most substantial fracture size is observed at an injection volume of 150 m³. Relative to the lowest injection rate, this configuration represents an increment of 0.6%, 2.0%, and 0.7%, respectively.

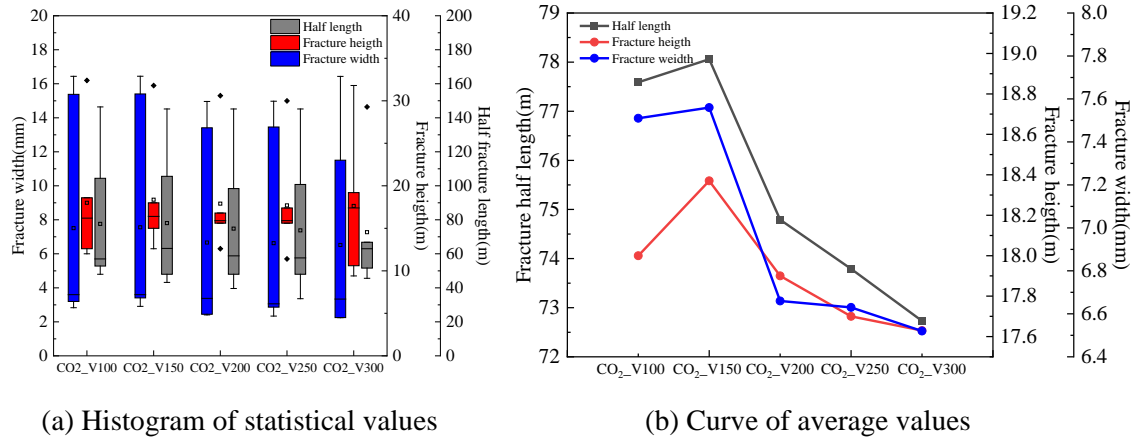


Figure 5. The fracture size under different CO₂ injection volume

The effect of pre-CO₂ injection volume on the S demonstrates a non-linear growth pattern. At an injection volume of 150 m³, the corresponding S value reaches 186432.8 m², presenting the most substantial rate of increase at 6.3%. On contrast, the D follows an initial rise succeeded by a subsequent decrease in relation to the injection volume. Notably, at an injection volume of 150 m³, D reaches its pinnacle value of 1.212. This signifies that under this specific condition, the fracture complexity is at its peak.

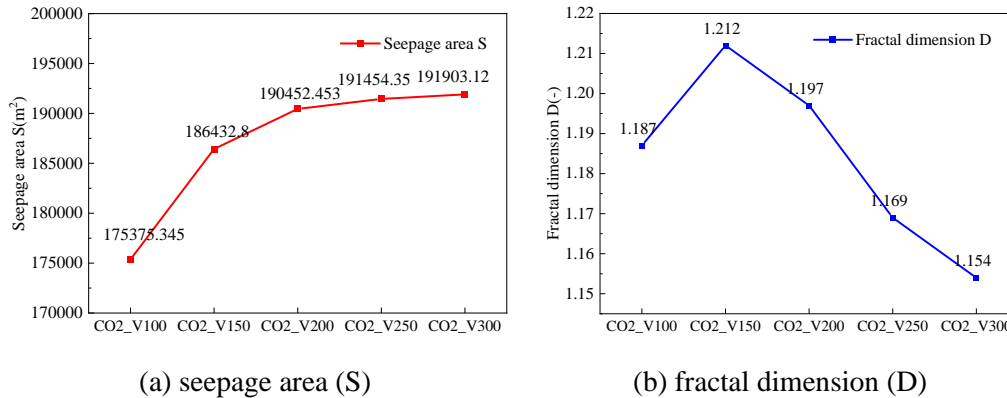


Figure 6. Seepage area and fractal dimension under different CO₂ injection volume

For instances where the injection volume remains relatively small, CO₂ predominantly accumulates in proximity to the injection port, limiting the scope of energy distribution within the formation. Owing to the shale reservoir's well-developed bedding, the

continual injection of pre-CO₂ leads to a progressive escalation in the number and complexity of fractures. This, in turn, elevates fluid leakage within fractures, subsequently diminishing the overall fracturing effect. This trend aligns with numerous prior studies [10, 11].

Fracturing Construction Parameter Design

Employing the S as the optimization criterion, a two-parameter fracturing construction chart is formulated, encompassing the pre-CO₂ injection volume and injection displacement. By amalgamating the findings from the preceding two sections, it becomes evident that an increase in injection displacement corresponds to a non-linear escalation in the S . Specifically, when the front CO₂ injection displacement ranges from 2 to 4 m³/min, and the injection volume ranges from 100 to 200 m³, the S attains a substantial value. In this case, the fractures exhibit the distinctive characteristics of being "short, high, and narrow".

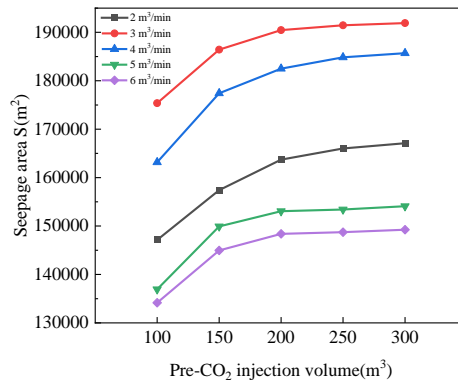


Figure 7. Fracturing construction parameter design chart

Conclusions

The mean half-length and width of fractures follow an initial growth and then decline trajectory in response to escalating pre-CO₂ injection displacement. Meanwhile, the fracture height exhibits a non-linear ascending pattern. The behavior of both the S and the D mirrors an initial increase followed by a subsequent decrease. The transformation of fracture shape progresses from "long, low, and wide" to "short, high, and narrow" with increasing injection displacement, concurrently exhibiting a declining trend in fracture complexity. During the fracturing stimulation phase of shale reservoirs, it is judicious to maintain a low pre-CO₂ injection displacement. The volume of pre-CO₂ injection exhibits minimal influence on the fracture propagation behavior. As pre-CO₂ injection volume increases, the fracture size displays an initial expansion followed by a subsequent non-linear reduction. Simultaneously, the S showcases a non-linear progression, while the D experiences an initial rise before subsequently diminishing with heightened injected volume. Utilizing the S as the guiding optimization criterion, we formulate a dual-parameter fracturing map that factors in both pre-CO₂ injection volume and injection displacement. This map is designed to offer valuable guidance for the future design of field construction parameters within shale reservoirs.

Acknowledgments

This study was funded by Science Foundation of China University of Petroleum, Beijing (2462021YXZZ009) and The Strategic Cooperation Technology Projects of CNPC and CUPB (ZLZX 2020-01) and Innovation Capability Support of Shaanxi Technical Innovation Team for Low Carbon Environmental Protection and Enhanced Oil Recovery in Unconventional

References

- [1] Smith, M. B., *et al.*, Hydraulic Fracturing, *Annual Review of Fluid Mechanics*, 47(2015), 2, pp. 124-135
- [2] Middleton, R. S., *et al.*, Shale Gas and Non-Aqueous Fracturing Fluids: Opportunities and Challenges for Supercritical CO₂, *Applied Energy*, 147(2015), 2, pp. 500-509
- [3] Wang, H. Z., *et al.*, Research Status and Prospects of Supercritical CO₂ Fracturing Technology, *Acta Petrolei Sinica*, 41(2020), 1, pp. 116-126
- [4] Middleton, R., *et al.*, CO₂ As A Fracturing Fluid: Potential for Commercial-Scale Shale Gas Production and CO₂ Sequestration, *Energy Procedia*, 63(2014), pp. 7780-7784
- [5] Xia, Y. L., *et al.*, Experimental and Numerical Study on Influencing Factors of Replacement Capacity and Slick Water Flowback Efficiency Using Pre-CO₂ Fracturing in Tight Oil Reservoirs, 215(2022), Article ID 110697
- [6] Zang, Y. X., *et al.*, In: SPE Gas & Oil Technology Showcase and Conference, *SPE*, (2023), pp. D021S033R005
- [7] Zang, Y. X., *et al.*, Laboratory Visualization of Supercritical CO₂ Fracturing in Tight Sandstone Using Digital Image Correlation Method, *Geoenergy Science and Engineering*, 225(2023), 6, Article ID 211556
- [8] A. Mukhamedzianova, GOHFER® software evaluation, *University of Leoben*, 2017
- [9] Barree, R. D., *et al.*, A Practical Numerical Simulator for Three-Dimensional Fracture Propagation in Heterogeneous Media, *SPE reservoir simulation symposium*, OnePetro, 1983
- [10] Schultz, R., *et al.*, Hydraulic Fracturing Volume Is Associated with Induced Earthquake Productivity in the Duvernay Play, *Science*, 359(2018), 1, pp. 304-308
- [11] Ji, Y. J., *et al.*, Effects of External Temperature and Dead Volume on Laboratory Measurements of Pore Pressure and Injected Volume in A Rock Fracture, *Journal of Rock Mechanics and Geotechnical Engineering*, 14(2022), 5, pp. 1461-1469

Paper submitted: June 12, 2023

Paper revised: August 21, 2023

Paper accepted: November 17, 2023